Alternating Ferro- and Antiferromagnetic Interactions in Unusual Copper(II) Chains

Giovanni De Munno,*,† Miguel Julve,*,‡ Francesc Lloret,‡ Juan Faus,‡ Michel Verdaguer,§ and Andrea Caneschi‖

Dipartimento di Chimica, Università della Calabria, 87030 Arcavacata di Rende, Cosenza, Italy, Departament de Química Inorgànica, Facultat de Química de la Universitat de València, Dr. Moliner 50, 46100 Burjassot, València, Spain, Laboratoire de Chimie des Métaux de Transition, URA CNRS 419, Université Pierre et Marie Curie, 4 Place Jussieu, 75252 Paris, France, and Dipartimento di Chimica, Università degli Studi di Firenze, 75/77 Via Maragliano, 50144 Firenze, Italy

Received August 30, 1994[⊗]

The preparation, the X-ray crystal structure, and the magnetic properties of four 2,2′-bipyrimidine ($C_8H_6N_4$, bpm)-containing copper(II) complexes of formula $[Cu_2(bpm)_2(H_2O)_2(OH)_2(NO_3)_2]\cdot4H_2O$ (**1**), $[Cu_2(bpm)(OH)_2(NO_3)_2]\cdot2H_2O$ (**2**), $[Cu_2(bpm)(H_2O)_2(OH)_2](NO_3)_2$ (**3**), and $[Cu_2(bpm)(H_2O)_2(OH)_2(NO_3)_2]\cdot2H_2O$ (**4**) are reported. Crystallographic data are as follows: **1**, triclinic system, space group $P\bar{1}$, $a = 7.703(1)$ Å, $b = 7.885(1)$ Å, $c = 11.172(2)$ Å, $\alpha = 87.29(1)°$, $\beta = 86.85(1)°$, $\gamma = 78.17(1)°$, $Z = 1$, $V = 662.7(2)$ Å^3; **2**, monoclinic system, space group $C2/c$, $a = 33.619(7)$ Å, $b = 13.040(3)$ Å, $c = 7.040(1)$ Å, $\beta = 101.90(3)°$, $Z = 8$, $V = 3019.8(10)$ Å^3; **3**, monoclinic system, space group $P2_1/n$, $a = 9.316(2)$ Å, $b = 8.286(2)$ Å, $c = 9.693(2)$ Å, $\beta = 90.52(2)°$, $Z = 2$, $V = 748.2(3)$ Å^3; **4**, triclinic system, space group $P\bar{1}$, $a = 7.564(2)$ Å, $b = 8.032(2)$ Å, $c = 8.238(2)$ Å, $\alpha = 61.33(2)°$, $\beta = 88.66(2)°$, $\beta = 88.66(2)°$, $\gamma = 75.97(2)°$, $Z = 1$, $V = 423.5(2)$ Å^3. The structure of **1** is made up of discrete, centrosymmetric bis(μ-hydroxo) copper(II) dimers with bpm as terminal ligand, weakly coordinated water molecules, unidentate nitrate anions, and molecules of water of crystallization. The copper environment in **1** is distorted octahedral with two bridging hydroxo groups and two nitrogen atoms of bpm building the equatorial plane whereas two oxygen atoms from water and nitrato groups occupy the axial positions. The Cu(1)−OH−Cu(1a) bridging angle is 95.7(1)°, and the intramolecular Cu(1)···Cu(1a) separation is 2.881(1) Å. The structures of **2**−**4** consist of cationic one-dimensional chains of copper(II) ions alternatively bridged by bpm and two hydroxo groups. The electroneutrality is achieved through unidentate (**2** and **4**) and uncoordinated (**3**) nitrate groups. Coordinated (**3** and **4**) and crystallization (**2** and **4**) water molecules are also present. The metal environment in **2** and **3** is square pyramidal, whereas it can be described as distorted octahedral in **4**. Copper atoms in **2**−**4** have in common the occurrence of two nitrogen atoms of bpm and two oxygen hydroxo groups in the equatorial plane, whereas the axial positions are occupied by oxygen atoms of nitrate (**2**), of water (**3**), and of both ligands (**4**). The angles at the hydroxo bridge for **2**−**4** vary in the range 95.0(1)−96.1(2)°, and they are very close to that of **1**. The metal−metal separations through the double-hydroxo bridge [2.886(1) (**2**), 2.854(1) (**3**), and 2.860(1) Å (**4**)] are much shorter than that through bis-chelating bpm [5.471(1) and 5.474(1) (**2**), 5.461(2) (**3**), and 5.452(2) Å (**4**)]. The magnetic properties of **1**−**4** have been investigated in the temperature range 4.2−300 K. A strong intramolecular ferromagnetic coupling (114 cm^{-1} for the singlet−triplet energy gap) is observed in **1**. Alternating antiferromagnetic ($-J$ = 145−135 cm^{-1}) interactions through the bpm bridge and ferromagnetic (αJ = 160−97.5 cm^{-1}) interactions through the hydroxo bridge are obtained for **2**−**4** by analyzing the magnetic susceptibility data with the Hamiltonian $\hat{H} = -J\sum(\hat{S}_{2i}\hat{S}_{2i-1} - \alpha\hat{S}_{2i}\hat{S}_{2i+1})$. These values are discussed in the light of the structural features and correlated with previously reported bpm- and double hydroxide-bridged copper(II) complexes.

Introduction

One-dimensional magnetic systems have been thoroughly investigated from both experimental and theoretical viewpoints.[1,2] In this area, studies of antiferromagnetic alternating chains have been particularly fruitful.[3] Two antiferromagnetic J_i and J_{i+1} coupling constants with an alternation parameter $\alpha = J_i/J_{i+1}$ generally occur in this kind of systems. The regular alternation of the intrachain exchange coupling interactions is achieved either by alternating the bridging ligands between the metal ions in a ...−L−M−L′−M−L−... sequence (safe synthetic route based on the coordinating capability of the bridging ligands) or by alternating spacing (more hazardous procedure, given the difficulty to master the stacking of the mononuclear or dinuclear precursors). The large number of antiferromagnetic alternating chains contrasts with the paucity of alternating chains with J_i and J_{i+1} of different sign (ferro- and antiferromagnetic). The best documented systems are $CuCl_3\cdot$(4-Bzpip) (Bzpip =

† Università della Calabria.
‡ Universitat de València.
§ Université Pierre et Marie Curie.
‖ Università degli Studi di Firenze.
⊗ Abstract published in *Advance ACS Abstracts*, December 1, 1994.

(1) (a) *Extended Linear Chain Compounds*; Miller, J. S., Ed.; Plenum: New York, 1983. (b) Bonner, J. C. In *Magneto-Structural Correlations in Exchange Coupled Systems*; Willett, R. D., Gatteschi, D., Kahn, O., Eds.; NATO ASI Series 140; Reidel: Dordrecht, The Netherlands, 1985; p 157. (c) *Organic and Inorganic Low-Dimensional Crystalline Materials*; Delhaes, P., Drillon, M., Eds.; NATO ASI Series 168; Plenum: New York, 1987.
(2) *Magnetic Molecular Materials*; Gatteschi, D., Kahn, O., Miller, J. S., Palacio, F., Eds.; Kluwer Academic Publishers: Dordrecht, The Netherlands, 1991.
(3) Landee, C. P. In *Organic and Inorganic Low-Dimensional Crystalline Materials*; Delhaes, P., Drillon, M., Eds.; NATO ASI Series 168; Plenum: New York, 1987; p 75.

0020-1669/95/1334-0157$09.00/0

4-benzylpiperidinium),[4] Cu(hfac)·TEMPOL (hfac = hexafluoroacetylacetonate and TEMPOL = 4-hydroxy-2,2,6,6-tetramethylpiperidinyl-*N*-oxy),[5] and Cu(TIM)$CuCl_4$ (TIM = 2,3,9,10-tetramethyl-1,3,8,10-tetraenecyclo-1,4,8,11-tetraazatetradecane)[6] which have (J_1, J_2) values estimated to be (42, -4.2 cm^{-1}), (25.8, -0.1 cm^{-1}), and (9.2, -1.8 cm^{-1}), respectively. The difficulties are associated not only with the design of ferromagnetically coupled dimers[7] but also with their polymerization through bridging ligands which mediate interdimer antiferromagnetic coupling, hence the small number of such compounds.

Simple ligands such as hydroxo bridges could be very appropriate to build one-dimensional magnetic systems with regular alternation of ferro- and antiferromagnetic couplings. In this respect, it is well-known that bis(μ-hydroxo)dicopper(II) complexes $[LCu(OH)_2CuL]^{2+}$ with a Cu(OH)Cu bridging angle θ smaller than 97.5° are ferromagnetically coupled.[8,9] The triplet state is the low-lying state when a bidentate N-donor such as 2,2′-bipyridine (bpy) is used as the outer ligand.[9,10] If 2,2′-bipyrimidine (hereafter noted bpm) is used instead of bpy, the resulting ferromagnetically coupled dinuclear unit[11] can be used as a complex ligand toward transition metal ions to build alternating chains by taking advantage of the bis-chelating character of bpm. Given that bpm is able to mediate antiferromagnetic interactions between transition metal ions when acting as a bridging ligand,[12,13] the resulting unusual chains would exhibit a regular alternation of ferro- and antiferromagnetic interactions.

We therefore synthesized the dinuclear copper(II) precursor of formula $[Cu_2(bpm)_2(H_2O)_2(OH)_2(NO_3)_2]\cdot4H_2O$ (**1**) and the related one-dimensional copper(II) compounds $[Cu_2(bpm)(OH)_2(NO_3)_2]\cdot2H_2O$ (**2**), $[Cu_2(bpm)(H_2O)_2(OH)_2](NO_3)_2$ (**3**), and $[Cu_2(bpm)(H_2O)_2(OH)_2(NO_3)_2]\cdot2H_2O$ (**4**). In the present work we report their preparations, crystal structure determinations, and magnetic characterizations. A preliminary communication concerning the structure and magnetic investigation of compounds **1** and **2** was published elsewhere.[14]

Experimental Section

General Information. All reagents were commercial grade materials, used as received. 2,2′-Bipyrimidine was purchased from Lancaster Synthesis. Elemental analyses (C, H, N) were carried out by the Microanalytical Service from the Universidad Autónoma de Madrid. Copper contents were determined by absorption spectrometry.

Preparation of Complex 1. This compound was obtained as follows: Solid sodium carbonate (0.5 mmol) was slowly added under continuous stirring to an aqueous solution (60 mL) containing copper(II) nitrate trihydrate (1 mmol) and bpm (1 mmol). After some precipitate was filtered out, the dark blue solution was allowed to evaporate at room temperature. After several days, blue-green rhombohedral crystals of **1** formed. They were filtered off and air-dried (yield about 90%). The most relevant features of the IR spectrum of **1** concern the occurrence of the $Cu(OH)_2Cu$ unit and chelating bpm. The former is supported by the presence of a weak and sharp peak at 3520 cm^{-1} (bridging OH stretching) and a weak absorption at 940 cm^{-1} (OH bending vibration).[15,16] The latter is suggested by the appearance of two intense and sharp peaks of nearly equal intensities at 1580 and 1560 cm^{-1} (ring stretching modes of bpm).[11,13b] Anal. Calcd for $[Cu_2(bpm)_2(H_2O)_2(OH)_2(NO_3)_2]\cdot4H_2O$ (**1**): C, 27.1; H, 3.67; N, 19.74; Cu, 17.92. Found: C, 26.98; H, 3.54; N, 19.65; Cu, 17.67.

Preparation of Complex 2. A mixture of **1** and green chunky single crystals of **2** was obtained by slow evaporation of dark blue aqueous solutions (80 mL) containing copper(II) nitrate trihydrate (2 mmol), bpm (1 mmol), and sodium carbonate (1 mmol). The yield was low because of the initial precipitation of some copper(II) hydroxide. Crystals of **2** were hand-picked, air-dried, and checked by X-ray diffraction. The synthesis was repeated until the required amount of **2** to make magnetic measurements and elemental analysis was obtained. The presence of a very asymmetric doublet (sharp and strong absorption at 1585 cm^{-1} and a weak peak at 1565 cm^{-1}) in the IR spectra of **2** (and also of **3** and **4**) is indicative of the occurrence of bis-chelating bpm.[13b] Anal. Calcd for $[Cu_2(bpm)(OH)_2(NO_3)_2]\cdot2H_2O$ (**2**): C, 20.05; H, 2.50; N, 17.53; Cu, 26.52. Found: C, 19.93; H, 2.41; N, 17.35; Cu, 26.38.

Preparation of Complexes 3 and 4. Solid sodium carbonate (0.5 mmol) was slowly added with stirring to an aqueous solution (150 mL) containing copper(II) nitrate trihydrate (1.9 mmol) and bpm (1.63 mmol). A blue greenish crystalline powder, which separated first from the resulting dark blue solution by slow evaporation at room temperature, was filtered off and discarded. A mixture of light blue polyhedral crystals of **4** (main product) and dark blue prismatic crystals of **3** (a small amount) was obtained from the mother liquor after a week. They were separated manually, air-dried, and checked by X-ray diffraction. Anal. Calcd for $[Cu_2(bpm)(H_2O)_2(OH)_2](NO_3)_2$ (**3**): C, 20.05; H, 2.50; N, 17.53; Cu, 26.52. Found: C, 19.78; H, 2.35; N, 17.40; Cu, 26.30. Anal. Calcd for $[Cu_2(bpm)(H_2O)_2(OH)_2(NO_3)_2]\cdot2H_2O$ (**4**): C, 18.65; H, 3.11; N, 16.31; Cu, 24.67. Found: C, 18.55; H, 3.02; N, 16.23; Cu, 24.48.

Instrumentation. IR spectra (KBr pellets) were taken on a Perkin-Elmer 1750 FTIR spectrometer. Variable-temperature X-ban EPR spectra were recorded on polycrystalline samples with Bruker ER 200D (**1**) and Varian E-9 (**2**–**4**) spectrometers equipped with helium cryostats. The magnetic susceptibilities were measured in the temperature range 4–300 K with a fully automated AZTEC DSM8 pendulum-type susceptometer (**1** and **4**) equipped with a TBT continuous-flow cryostat and a Bruker BE15 electromagnet operating at 1.8 T and a Metronique Ingenierie MS03 SQUID magnetometer (**2** and **3**). The instruments were calibrated with $Hg[Co(NCS)_4]$. Corrections for the diamagnetism

(4) De Groot, H. J. M.; de Jongh, L. J.; Willett, R. D.; Reedijk, *J. Appl. Phys.* **1982**, *53*, 8038.
(5) Benelli, C.; Gatteschi, D.; Carnegie, D. W.; Carlin, R. L. *J. Am. Chem. Soc.* **1985**, *107*, 2560.
(6) Vasilevesky, I.; Rose, N. R.; Stenkamp, R.; Willett, R. D. *Inorg. Chem.* **1991**, *30*, 4082.
(7) Kahn, O. *Comments Inorg. Chem.* **1984**, *3*, 105.
(8) Hatfield, W. E. In *Magneto-Structural Correlations in Exchange Coupled Systems*; Willett, R. D., Gatteschi, D., Kahn, O., Eds.; NATO ASI Series 140; Reidel: Dordrecht, The Netherlands, 1985; p 555 and references therein.
(9) Crawford, V. H.; Richardson, H. W.; Wasson, J. R.; Hodgson, D. J.; Hatfield, W. E. *Inorg. Chem.* **1976**, *15*, 2107.
(10) (a) Majeste, R. J.; Meyers, E. A. *J. Phys. Chem.* **1970**, *74*, 3497. (b) McGregor, K. T.; Watkins, N. T.; Lewis, D. L.; Drake, R. F.; Hodgson, D. J.; Hatfield, W. E. *Inorg. Nucl. Chem. Lett.* **1973**, *9*, 423. (c) Toofan, M.; Bousheri, M.; Ul-Haque, M. *J. Chem. Soc., Dalton Trans.* **1976**, 217. (d) Casey, A. T.; Hoskins, B. F.; Whillans, F. D. *Chem. Commun.* **1970**, 904. (e) Hoskins, B. F.; Whillans, F. D. *J. Chem. Soc., Dalton Trans.* **1975**, 1267. (f) McGregor, K. T.; Hodgson, D. J.; Hatfield, W. E. *Inorg. Chem.* **1972**, *12*, 731. (g) Castro, I.; Faus, J.; Julve, M.; Verdaguer, M.; Monge, A.; Gutiérrez-Puebla, E. *Inorg. Chim. Acta* **1990**, *170*, 251. (h) Sletten, J.; Sørensen, A.; Julve, M.; Journaux, Y. *Inorg. Chem.* **1990**, *29*, 5054. (i) Castro, I.; Faus, J.; Julve, M.; Bois, C.; Real, J. A.; Lloret, F. *J. Chem. Soc., Dalton Trans.* **1992**, 47.
(11) Castro, I.; Julve, M.; De Munno, G.; Bruno, G.; Real, J. A.; Lloret, F.; Faus, J. *J. Chem. Soc., Dalton Trans.* **1992**, 1739.
(12) Brewer, G.; Sinn, E. *Inorg. Chem.* **1985**, *24*, 4580.
(13) (a) Julve, M.; De Munno, G.; Bruno, G.; Verdaguer, M. *Inorg. Chem.* **1988**, *27*, 3160. (b) Julve, M.; Verdaguer, M.; De Munno, G.; Real, J. A.; Bruno, G. *Inorg. Chem.* **1993**, *32*, 795. (c) Andrés, E.; De Munno, G.; Julve, M.; Real, J. A.; Lloret, F. *J. Chem. Soc., Dalton Trans.* **1993**, 2169.
(14) De Munno, G.; Julve, M.; Lloret, F.; Faus, J.; Verdaguer, M.; Caneschi, A. *Angew. Chem., Int. Ed. Engl.* **1993**, *32*, 1046.
(15) Ferraro, J. R.; Walker, W. R. *Inorg. Chem.* **1965**, *4*, 1382.
(16) Nakamoto, K. *Infrared and Raman Spectra of Inorganic and Coordination Compounds*, 4th ed.; Wiley: New York, 1986; p 230 and references therein.

Table 1. Crystallographic Data for Compounds **1−4**

	1	2	3	4
formula	$C_{16}H_{26}Cu_2N_{10}O_{14}$	$C_8H_{12}Cu_2N_6O_{10}$	$C_8H_{12}Cu_2N_6O_{10}$	$C_8H_{16}N_6Cu_2O_{12}$
fw	709.5	479.3	479.3	515.3
space group	$P\bar{1}$	$C2/c$	$P2_1/n$	$P\bar{1}$
a, Å	7.703(1)	33.619(7)	9.316(2)	7.564(2)
b, Å	7.885(1)	13.040(3)	8.286(2)	8.032(2)
c, Å	11.172(2)	7.040(1)	9.693(2)	8.238(2)
α, deg	87.29(1)			61.33(2)
β, deg	86.85(1)	101.90(3)	90.52(2)	88.66(2)
γ, deg	78.17(1)			75.97(2)
V, Å^3	662.7(2)	3019.8(10)	748.2(3)	423.5(2)
Z	1	8	2	1
d_{calc}, g cm^{-3}	1.778	2.109	2.128	2.021
μ(Mo Kα), cm^{-1}	16.91	28.93	29.14	25.90
R^a	0.030	0.041	0.038	0.034
$R_w{}^b$	0.035	0.047	0.041	0.034

^{a} $R = \Sigma||F_o| - |F_c||/\Sigma|F_o|$. ^{b} $R_w = [\Sigma(||F_o| - |F_c||)^2/\Sigma wF_o^2]^{1/2}$.

of the complexes **1−4** were estimated from Pascal's constants[17] as -362×10^{-6}, -210×10^{-6}, -210×10^{-6}, and -236×10^{-6} cm^3 mol^{-1}, respectively.

Crystallographic Structure Determinations. X-ray data for complexes **1−4** were collected at 298 K with a Siemens R3mV automatic four-circle diffractometer by using graphite-monochromated Mo Kα radiation (λ = 0.710 73 Å). Crystals of **1−4** of dimensions 0.21 × 0.19 × 0.45, 0.27 × 0.10 × 0.08, 0.14 × 0.16 × 0.32, and 0.08 × 0.09 × 0.11 mm^3, respectively, were used. Accurate unit-cell dimensions and crystal orientation matrices were obtained from least-squares refinement of the setting angles of 25 reflections in the $15 \le 2\theta \le 30°$ range. Crystallographic data and details of the refinement are reported in supplementary Table S1 and in a condensed form in Table 1. The crystal data for compounds **1** and **2** have been previously reported,[14] and their atomic coordinates, bond lengths and angles, and thermal parameters have been deposited at the Fachinformationszentrum Karlsruhe (FRG). $\omega-2\theta$ (**1**, **3**, and **4**) and ω (**2**) scan techniques were used during data collection. Examination of three standard reflections, monitored every 100, showed no sign of crystal deterioration. Data were corrected for Lorentz and polarization effects. ψ-Scan absorption correction was used for compounds **1**, **2**, and **4**,[18] whereas data for **3** were corrected by using the XABS program.[19] Of the 3167 measured reflections for **1**, 2673 were unique with $I > 3\sigma(I)$, while these numbers were 21 678 and 2032 for **2**, 1924 and 1110 for **3**, and 2008 and 1513 for **4**. The maximum and minimum transmission factors were 0.585 and 0.485 for **1**, 0.595 and 0.486 for **2**, 0.769 and 0.413 for **3**, and 0.509 and 0.393 for **4**.

The structures were solved by standard Patterson methods and subsequently completed by Fourier recycling. All non-hydrogen atoms were refined anisotropically. The hydrogen atoms of the water molecules and OH groups were located on a ΔF map and refined with constraints. The hydrogen atoms of bpm were set in calculated positions and refined as riding atoms. A common thermal parameter was assigned to all hydrogen atoms. The final full-matrix least-squares refinement, minimizing the function $\Sigma w(||F_o| - |F_c||)^2$ with $w = 1/[\sigma^2(F_o) + qF_o^2]$ [q = 0.0020 (**1**), 0.0034 (**2**), and 0.0010 (**3**, **4**)] converged to final residuals R (R_w) of 0.0304 (0.0351) for **1**, 0.0413 (0.0473) for **2**, 0.0378 (0.0407) for **3**, and 0.0337 (0.0341) for **4**. In the final difference map the residual maxima and minima were 0.35 and −0.84 (**1**), 1.14 and −0.67 (**2**), 0.76 and −0.60 (**3**), and 0.59 and −1.15 e Å^{-3} (**4**). The largest and mean Δ/σ are 0.561 and 0.038 for **1**, 0.063 and 0.006 for **2**, 0.108 and 0.007 for **3** and 0.112 and 0.005 for **4**. Solutions and refinements were performed with the SHELXTL-PLUS system,[19] final geometrical calculations with the PARST program,[20] and graphical manipulations using the XP utility of the SHELXTL-PLUS system. Positional parameters for non-hydrogen atoms of **1−4** are listed in Tables 2−5, respectively. Main interatomic bond distances and angles are given in Tables 6 (**1**), 7 (**2**), 8 (**3**), and 9 (**4**). Anisotropic temperature factors (Tables S2−S5 for **1−4**), hydrogen atom coordinates (Tables S6−S9 for **1−4**), nonessential bond lengths and angles (Tables S10−S13 for **1−4**), and least-squares planes (Tables S14−S17 for **1−4**) are available as supplementary material.

(17) Earnshaw, A. *Introduction to Magnetochemistry*; Academic Press: London and New York, 1968.
(18) North, A. C. T.; Phillips, D. C.; Mathews, F. S. *Acta Crystallogr., Sect. C*, **1968**, *24*, 351.
(19) *SHELXTL PLUS*, Version 4.21/V; Siemens Analytical X-ray Instruments Inc.: Madison, WI, 1990.
(20) Nardelli, M. *Comput. Chem.* **1983**, *7*, 95.

Table 2. Final Atomic Fractional Coordinates^a and Equivalent Isotropic Displacement Parameters^b for **1**

atom	x	y	z	U_{eq}, Å^2
Cu(1)	0.0175(1)	0.1047(1)	0.3926(1)	0.024(1)
N(1)	0.1914(2)	0.2421(2)	0.3176(2)	0.027(1)
N(2)	−0.0717(2)	0.1397(2)	0.2249(2)	0.027(1)
N(3)	0.2655(3)	0.3773(3)	0.1328(2)	0.037(1)
N(4)	−0.0085(3)	0.2614(2)	0.0332(2)	0.033(1)
N(5)	0.3953(2)	−0.1342(2)	0.2896(2)	0.036(1)
O(1)	0.1310(2)	0.0538(2)	0.5450(1)	0.028(1)
O(2)	−0.1950(2)	0.3378(2)	0.4570(2)	0.039(1)
O(3)	0.0704(3)	0.3868(2)	0.6428(2)	0.054(1)
O(4)	0.2472(3)	0.3918(3)	0.8513(2)	0.057(1)
O(5)	0.2467(2)	−0.1697(3)	0.3033(2)	0.048(1)
O(6)	0.4793(3)	−0.1119(3)	0.3769(2)	0.063(1)
O(7)	0.4557(3)	−0.1079(3)	0.1859(2)	0.064(1)
C(1)	0.3247(3)	0.2919(3)	0.3693(2)	0.033(1)
C(2)	0.4331(3)	0.3868(3)	0.3038(2)	0.040(1)
C(3)	0.3976(3)	0.4256(3)	0.1857(2)	0.042(1)
C(4)	0.1694(3)	0.2869(2)	0.2014(2)	0.027(1)
C(5)	0.0207(3)	0.2269(2)	0.1485(2)	0.026(1)
C(6)	−0.1456(3)	0.2062(3)	−0.0079(2)	0.037(1)
C(7)	−0.2492(3)	0.1158(3)	0.0638(2)	0.039(1)
C(8)	−0.2090(3)	0.0828(3)	0.1833(2)	0.034(1)

^{a} Estimated standard deviations in the last significant digits are given in parentheses. ^{b} U_{eq} is defined as one-third of the trace of the orthogonalized $\mathbf{U}_{ij}$ tensor.

Results and Discussion

Description of the Structures. [$Cu_2(bpm)_2(H_2O)_2(OH)_2(NO_3)_2$]·$4H_2O$ (1). The structure of complex **1** is made up of discrete centrosymmetric bis(μ-hydroxo) copper(II) dimers, with bpm as the terminal bidentate ligand, weakly coordinated water molecules and unidentate nitrate groups, and crystallization water molecules. A perspective view of this complex, with the atom-numbering scheme, is depicted in Figure 1. An extensive network of hydrogen bonds (see end of Table 6) links both coordinated and crystallization water molecules and nitrate anions, most of them being represented by broken lines in Figure 1.

Each copper atom has a distorted 4+1+1 elongated tetragonal octahedral coordination, as in the parent [$Cu_2(bpm)_2(H_2O)_4(OH)_2$]($ClO_4$)$_2$·$2H_2O$ (**5**).[11] In both complexes, the four equatorial positions are occupied by two nitrogen atoms of bpm and

Table 3. Final Atomic Fractional Coordinates[a] and Equivalent Isotropic Displacement Parameters[b] for **2**

atom	x	y	z	U_{eq}, Å^2
Cu(1)	0.4185(1)	0.2663(1)	0.2462(1)	0.021(1)
Cu(2)	0.3314(1)	0.2607(1)	0.1588(1)	0.022(1)
O(1)	0.3742(1)	0.3593(3)	0.1577(6)	0.025(1)
O(2)	0.3760(1)	0.1648(3)	0.2045(7)	0.024(1)
N(1)	0.4645(1)	0.3701(4)	0.2470(7)	0.024(2)
C(1)	0.4641(2)	0.4728(5)	0.2443(10)	0.031(2)
C(2)	0.5000	0.5269(6)	0.2500	0.035(3)
C(3)	0.5000	0.3249(6)	0.2500	0.021(2)
C(4)	0.5000	0.2117(6)	0.2500	0.018(2)
C(5)	0.5000	0.0088(6)	0.2500	0.033(3)
C(6)	0.4648(2)	0.0631(4)	0.2569(10)	0.029(2)
N(2)	0.4648(1)	0.1648(3)	0.2559(7)	0.021(1)
N(3)	0.2866(1)	0.1534(4)	0.0959(8)	0.023(1)
C(7)	0.2875(2)	0.0518(4)	0.1217(10)	0.028(2)
C(8)	0.2530(2)	−0.0074(5)	0.0668(10)	0.030(2)
C(9)	0.2508(2)	0.1938(4)	0.0135(9)	0.019(2)
N(4)	0.2841(1)	0.3567(3)	0.0431(7)	0.022(1)
C(10)	0.2823(2)	0.4592(5)	0.0172(10)	0.031(2)
N(5)	0.4352(3)	0.2476(5)	0.6938(10)	0.050(3)
O(3)	0.4268(2)	0.3097(4)	0.5684(8)	0.069(3)
O(4)	0.4419(4)	0.2666(7)	0.8654(10)	0.121(5)
O(5)	0.4277(3)	0.1528(6)	0.6379(12)	0.107(4)
N(6)	0.3130(3)	0.2444(5)	0.5687(11)	0.061(3)
O(6)	0.3183(2)	0.3094(5)	0.4569(9)	0.072(3)
O(7)	0.3269(3)	0.1544(6)	0.5328(12)	0.096(4)
O(8)	0.3031(5)	0.2512(7)	0.7156(15)	0.158(7)
O(9)	0.3711(2)	0.5535(4)	0.2984(9)	0.047(2)
O(10)	0.3779(20)	−0.0369(4)	0.3806(8)	0.049(2)

[a] Estimated standard deviations in the last significant digits are given in parentheses. [b] U_{eq} is defined as one-third of the trace of the orthogonalized $\mathbf{U}_{ij}$ tensor.

Table 4. Final Atomic Fractional Coordinates[a] and Equivalent Isotropic Displacement Parameters[b] for **3**

atom	x	y	z	U_{eq}, Å^2
Cu(1)	0.0167(1)	0.1711(1)	0.4946(1)	0.024(1)
O(1)	0.0438(4)	0.0003(4)	0.6264(3)	0.029(1)
O(2)	0.2490(4)	0.1768(5)	0.4085(4)	0.037(1)
N(1)	0.0448(4)	0.3564(5)	0.6294(4)	0.023(1)
C(1)	0.0874(5)	0.3541(6)	0.7627(5)	0.026(1)
C(2)	0.1069(6)	0.4960(6)	0.8342(5)	0.030(1)
C(3)	0.0810(5)	0.6402(5)	0.7669(5)	0.027(1)
N(2)	0.0371(4)	0.6416(5)	0.6346(4)	0.023(1)
C(4)	0.0212(5)	0.4984(6)	0.5742(4)	0.020(1)
N(3)	0.3259(5)	0.5821(6)	0.4437(5)	0.037(2)
O(3)	0.3120(5)	0.4945(5)	0.3357(4)	0.051(1)
O(4)	0.3145(6)	0.7294(6)	0.4301(5)	0.065(2)
O(5)	0.3450(5)	0.5158(5)	0.5565(4)	0.047(1)

[a] Estimated standard deviations in the last significant digits are given in parentheses. [b] U_{eq} is defined as one-third of the trace of the orthogonalized $\mathbf{U}_{ij}$ tensor.

two oxygen atoms of the bridging hydroxo groups, whereas the axial sites are filled by a water molecule and a unidentate nitrate ligand in **1** and by two water molecules in **5**. The four equatorial bonds to copper occur in two sets: the Cu−N(bpm) and the Cu−O(hydroxo bridge), which average 2.016 and 1.944 Å, respectively. These values are very close to those found in **5** (2.021 and 1.947 Å). The four equatorial atoms are practically coplanar, with deviations from the least-squares plane lower than 0.06 Å, the copper atom being displaced 0.122(1) Å (0.064 (1) Å in **5**) toward the axial O(2) oxygen atom of the water molecule. The two Cu−O axial bonds are much longer [2.310(2) and 2.691(2) Å for Cu(1)−O(2) and Cu(1)−O(5), respectively] than the equatorial metal-to-ligand distances. The calculated tetragonality[21] is 0.79.

(21) Procter, I. M.; Hathaway, B. J.; Nicholls, P. J. *Chem. Soc. A* **1968**, 1678.

Table 5. Final Atomic Fractional Coordinates[a] and Equivalent Isotropic Displacement Parameters[b] for **4**

atom	x	y	z	U_{eq}, Å^2
Cu(1)	0.4897(1)	0.1804(1)	0.3321(1)	0.020(1)
O(1)	0.3618(3)	−0.0252(3)	0.4291(3)	0.022(1)
O(2)	0.2774(4)	0.3698(4)	0.4245(3)	0.034(1)
N(1)	0.3572(4)	0.3351(4)	0.0693(3)	0.020(1)
C(1)	0.2140(5)	0.3111(5)	−0.0018(4)	0.025(1)
C(2)	0.1374(5)	0.4436(5)	−0.1845(4)	0.027(1)
C(3)	0.2143(4)	0.5971(5)	−0.2888(4)	0.023(1)
N(2)	0.3600(3)	0.6190(4)	−0.2170(3)	0.020(1)
C(4)	0.4220(4)	0.4875(4)	−0.0411(4)	0.016(1)
N(3)	0.8548(4)	0.0318(4)	0.1855(4)	0.030(1)
O(3)	0.8660(4)	0.1679(5)	0.0267(4)	0.045(1)
O(4)	0.7219(4)	−0.0408(4)	0.2090(4)	0.044(1)
O(5)	0.9663(4)	−0.0189(5)	0.3191(4)	0.056(2)
O(6)	0.3862(4)	0.7147(4)	0.2815(4)	0.043(1)

[a] Estimated standard deviations in the last significant digits are given in parentheses. [b] U_{eq} is defined as one-third of the trace of the orthogonalized $\mathbf{U}_{ij}$ tensor.

Table 6. Selected Interatomic Bond Distances (Å), Angles (deg), and Hydrogen-Bonding Interactions for **1**[a]

Distances			
Cu(1)−N(1)	2.014(2)	Cu(1)−O(1a)	1.943(2)
Cu(1)−N(2)	2.018(2)	Cu(1)−O(2)	2.310(2)
Cu(1)−O(1)	1.944(2)	Cu(1)−O(5)	2.691(2)
Angles			
N(1)−Cu(1)−N(2)	80.7(1)	N(2)−Cu(1)−O(5)	84.7(1)
N(1)−Cu(1)−O(1)	96.1(1)	O(1)−Cu(1)−O(1a)	84.3(1)
N(1)−Cu(1)−O(1a)	172.5(1)	O(1)−Cu(1)−O(2)	95.9(1)
N(1)−Cu(1)−O(2)	97.1(1)	O(1)−Cu(1)−O(5)	88.4(1)
N(1)−Cu(1)−O(5)	84.3(1)	O(1a)−Cu(1)−O(2)	90.3(1)
N(2)−Cu(1)−O(1a)	98.0(1)	O(1a)−Cu(1)−O(5)	88.2(1)
N(2)−Cu(1)−O(1)	172.7(1)	O(2)−Cu(1)−O(5)	175.3(1)
N(2)−Cu(1)−O(2)	91.0(1)	Cu(1)−O(1)−Cu(1a)	95.7(1)

Hydrogen Bonds[b]

A	D	H	A···D, Å	A···H−D, deg
O(1)	O(3)	H(3w)	2.83(1)	177(2)
O(4)	O(3)	H(4w)	2.77(1)	167(3)
O(5a)	O(2)	H(2w)	2.97(1)	152(2)
O(7b)	O(4)	H(5w)	2.88(1)	158(2)
O(3c)	O(2)	H(1w)	2.72(1)	149(2)

[a] Symmetry operations: (a) $-x, -y, 1-z$; (b) $1-x, -y, 1-z$; (c) $-x, 1-y, 1-z$. [b] A = acceptor, D = donor.

The two pyrimidyl rings of bpm are planar, and they form a dihedral angle of 1.4(1)°. The two bpm molecules coordinated to Cu(1) and Cu(1a) atoms, and related by an inversion center, are on parallel planes 0.573(2) Å apart. The dihedral angle between the equatorial N(1)N(2)O(1)O(1a) and bpm mean planes is 5.5(1)°. The bond distances and angles within the bipyrimidine ligand are in agreement with those previously reported for free[22] and chelating[11,13b,23] bpm. The value of the angle subtended at the copper atom by bpm (80.7(1)° for N(1)-Cu(1)N(2)) departs significantly from 90°, due to the steric requirements of the bipyrimidyl ring system. This value is practically identical with that found for the same angle (80.3(1)°) in **5**.

The nitrate anion is planar, as expected. In addition to its unidentate coordination to the metal atom, the nitrate group contributes to the packing by forming hydrogen bonds involving two of its three oxygen atoms (Table 6). The values of the

(22) Fernholt, L.; Rømming, C.; Samdal, S. *Acta Chem. Scand., Ser. A* **1981**, *35*, 707.

(23) De Munno, G.; Bruno, G.; Julve, M.; Romeo, M. *Acta Crystallogr., Sect. C* **1990**, *46*, 1828. Morgan, L. W.; Pennington, W. T.; Petersen, J. D.; Ruminski, R. R.; Bennett, D. W.; Rommel, J. S. *Acta Crystallogr., Sect. C* **1992**, *48*, 163.

Table 7. Selected Interatomic Bond Distances (Å), Angles (deg), and Hydrogen-Bonding Interactions for **2**[a]

	Distances		
Cu(1)−N(1)	2.054(5)	Cu(2)−N(3)	2.036(5)
Cu(1)−N(2)	2.035(5)	Cu(2)−N(4)	2.055(5)
Cu(1)−O(1)	1.921(4)	Cu(2)−O(1)	1.931(4)
Cu(1)−O(2)	1.923(4)	Cu(2)−O(2)	1.930(4)
Cu(1)−O(3)	2.298(6)	Cu(2)−O(6)	2.320(7)
	Angles		
N(1)−Cu(1)−N(2)	81.8(2)	N(3)−Cu(2)−N(4)	81.7(2)
N(1)−Cu(1)−O(1)	96.7(2)	N(3)−Cu(2)−O(2)	96.0(2)
N(1)−Cu(1)−O(2)	171.1(2)	N(3)−Cu(2)−O(1)	167.2(2)
N(1)−Cu(1)−O(3)	84.1(2)	N(3)−Cu(2)−O(6)	96.6(2)
N(2)−Cu(1)−O(2)	95.6(2)	N(4)−Cu(2)−O(1)	96.3(2)
N(2)−Cu(1)−O(1)	163.3(2)	N(4)−Cu(2)−O(2)	166.6(2)
N(2)−Cu(1)−O(3)	101.0(2)	N(4)−Cu(2)−O(6)	85.2(2)
O(1)−Cu(1)−O(2)	83.4(2)	O(1)−Cu(2)−O(2)	82.9(2)
O(1)−Cu(1)−O(3)	95.4(2)	O(1)−Cu(2)−O(6)	95.9(2)
O(2)−Cu(1)−O(3)	104.8(2)	O(2)−Cu(2)−O(6)	108.2(2)
Cu(1)−O(1)−Cu(2)	96.2(2)	Cu(1)−O(2)−Cu(2)	96.1(2)

Hydrogen Bonds[b]

A	D	H	A···D, Å	A···H−D, deg
O(9)	O(1)	H(1o)	2.73(1)	150(5)
O(10)	O(2)	H(2o)	2.90(1)	137(4)
O(5c)	O(10)	H(3w)	3.03(1)	152(4)
O(1d)	O(9)	H(1w)	2.76(1)	147(5)
O(2e)	O(10)	H(4w)	2.84(1)	161(3)

[a] Symmetry operations: (a) $1/2 - x$, $1/2 - y$, $-z$; (b) $1 - x$, y, $1/2 - z$; (c) x, $-y$, $z - 1/2$; (d) x, $1 - y$, $z + 1/2$; (e) x, $-y$, $1/2 + z$. [b] A = acceptor, D = donor.

Table 8. Selected Interatomic Bond Distances (Å), Angles (deg), and Hydrogen-Bonding Interactions for **3**[a]

	Distances		
Cu(1)−N(1)	2.032(4)	Cu(1)−O(1b)	1.923(3)
Cu(1)−N(2a)	2.054(4)	Cu(1)−O(2)	2.326(4)
Cu(1)−O(1)	1.921(3)		
	Angles		
N(1)−Cu(1)−N(2a)	81.4(2)	N(2a)−Cu(1)−O(2)	89.4(1)
N(1)−Cu(1)−O(1)	96.5(1)	O(1)−Cu(1)−O(1b)	84.1(1)
N(1)−Cu(1)−O(1b)	170.3(2)	O(1)−Cu(1)−O(2)	97.9(1)
N(1)−Cu(1)−O(2)	95.8(1)	O(1b)−Cu(1)−O(2)	93.7(1)
N(2a)−Cu(1)−O(1b)	96.8(2)	Cu(1)−O(1)−Cu(1b)	95.9(1)
N(2a)−Cu(1)−O(1)	172.7(2)		

Hydrogen Bonds[b]

A	D	H	A···D, Å	A···H−D, deg
O(3)	O(2)	H(2w)	2.79(1)	171(5)
O(3c)	O(1)	H(1o)	2.98(1)	168(4)
O(3d)	O(2)	H(1w)	2.86(1)	156(5)

[a] Symmetry operations: (a) $-x$, $1 - y$, $1 - z$; (b) $-x$, $-y$, $1 - z$; (c) $x - 1/2$, $1/2 - y$, $1/2 + z$; (d) $1/2 - x$, $y - 1/2$, $1/2 - z$. [b] A = acceptor, D = donor.

intramolecular Cu(1)···Cu(1a) separation (2.881(1) Å) and the Cu(1)−O(1)−Cu(1a) bridging angle θ (95.7(1)°) are very close to those observed in **5** (2.870(1) Å and 95.0(1)°).

[Cu_2(bpm)$(OH)_2(NO_3)_2$]·$2H_2O$ (2), [Cu_2(bpm)$(H_2O)_2(OH)_2$]$(NO_3)_2$ (3), and [Cu_2(bpm)$(H_2O)_2(OH)_2(NO_3)_2$]·$2H_2O$ (4). The crystal structures of **2**−**4** consist of chains of copper(II) ions alternatively bridged by bpm and two hydroxo groups. The electroneutrality is achieved through unidentate (**2** and **4**) and uncoordinated (**3**) nitrate anions. Uncoordinated (**2**), coordinated (**3**), and both uncoordinated and coordinated water molecules (**4**) are also present. Compound **4** differs from **2** and **3** because there is an extra water molecule per metal atom. Perspective views of these alternating chains with the atom-numbering scheme are depicted in Figures 2 (top, **2**), 3 (top, **4**), and 4 (**4**).

Each copper atom in **2** and **3** has a distorted CuN_2O_3 square pyramidal coordination: two nitrogen atoms of bpm and two

Table 9. Selected Interatomic Bond Distances (Å), Angles (deg), and Hydrogen-Bonding Interactions for **4**[a]

	Distances		
Cu(1)−N(1)	2.038(2)	Cu(1)−O(1b)	1.938(2)
Cu(1)−N(2a)	2.039(3)	Cu(1)−O(2)	2.311(3)
Cu(1)−O(1)	1.942(3)	Cu(1)−O(4)	2.721(4)
	Angles		
N(1)−Cu(1)−N(2a)	81.8(1)	N(2a)−Cu(1)−O(4)	87.4(1)
N(1)−Cu(1)−O(1)	97.0(1)	O(1)−Cu(1)−O(1b)	85.0(1)
N(1)−Cu(1)−O(1b)	174.0(1)	O(1)−Cu(1)−O(2)	91.7(1)
N(1)−Cu(1)−O(2)	90.8(1)	O(1)−Cu(1)−O(4)	86.6(1)
N(1)−Cu(1)−O(4)	86.2(1)	O(1b)−Cu(1)−O(2)	94.8(1)
N(2a)−Cu(1)−O(1b)	95.6(1)	O(1b)−Cu(1)−O(4)	88.2(1)
N(2a)−Cu(1)−O(1)	173.9(1)	O(2)−Cu(1)−O(4)	176.3(1)
N(2a)−Cu(1)−O(2)	94.3(1)	Cu(1)−O(1)−Cu(1b)	95.0(1)

Hydrogen Bonds[b]

A	D	H	A···D, Å	A···H−D, deg
O(6)	O(2)	H(1w)	2.77(1)	145(3)
O(3a)	O(6)	H(4w)	2.83(1)	153(4)
O(4b)	O(2)	H(2w)	2.90(1)	164(2)
O(1c)	H(3w)	O(6)	2.85(1)	178(4)

[a] Symmetry operations: (a) $1 - x$, $1 - y$, $-z$; (b) $1 - x$, $-y$, $1 - z$; (c) x, $1 + y$, z. [b] A = acceptor, D = donor.

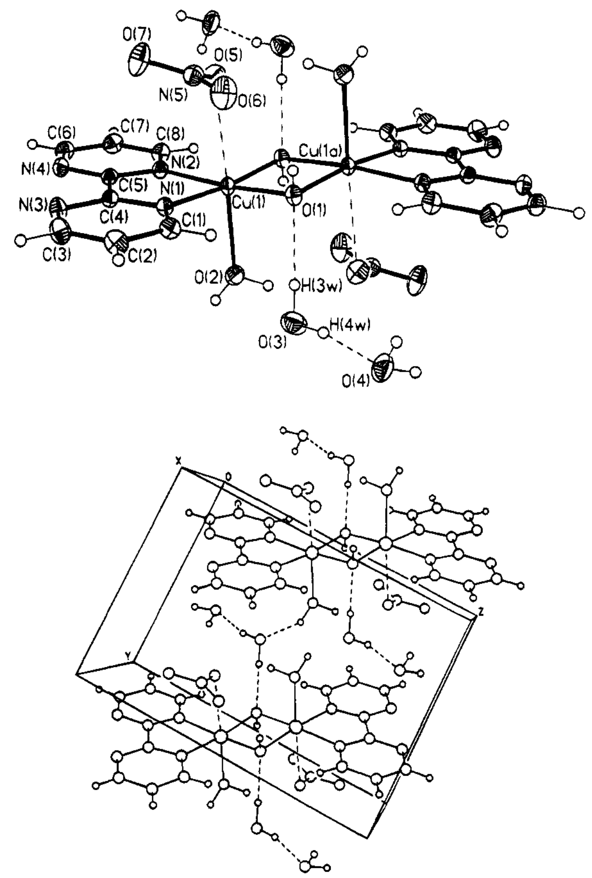

Figure 1. Crystal structure of **1**. Thermal ellipsoids are shown at the 30% probability level, whereas all hydrogen atoms are drawn with uniform isotropic thermal parameters; hydrogen bonds are depicted as broken lines. Top: ORTEP view of the dinuclear unit with the atom-numbering scheme. Bottom: View of the packing of the dinuclear units in the unit cell.

oxygen hydroxo groups form the equatorial plane in both compounds, whereas an oxygen atom of a nitrate anion (**2**) or of a water molecule (**3**) occupies the axial position. The Cu(1) and Cu(2) copper atoms in **2**, where a crystallographic inversion center is located at the middle of the C(9)−C(9a) bond and a two-fold axis passes through C(2), C(3), C(4), and C(5), are not equivalent (small differences appear in bond lengths and

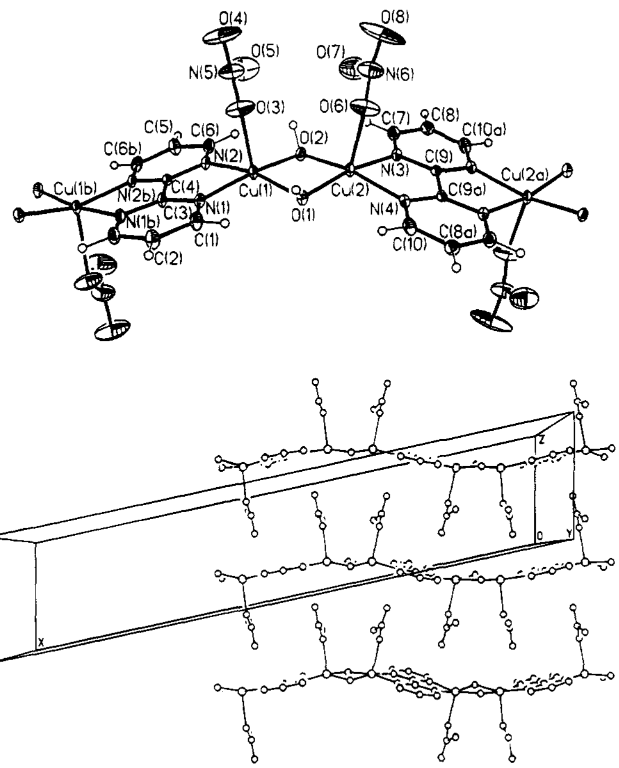

Figure 2. Crystal structure of **2**. Thermal ellipsoids are plotted at the 30% probability level. Top: ORTEP view of the alternating chain with the atom-numbering scheme. Bottom: Arrangement of the chains in the *xz* plane (hydrogen atoms and water molecules omitted for the sake of clarity).

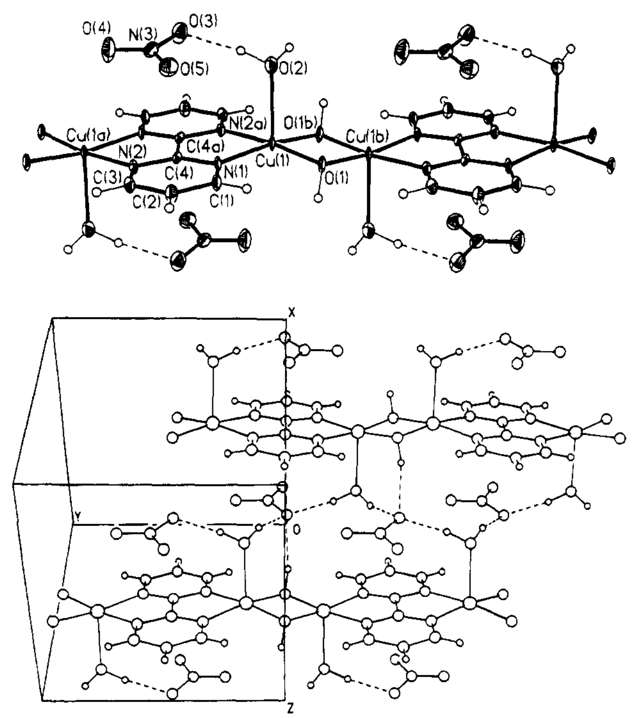

Figure 3. Crystal structure of **3**. Thermal ellipsoids are drawn at the 30% probability level. Top: ORTEP view of the alternating chain with the atom-numbering scheme. Bottom: View of the arrangement of the chains running parallel to the *b* axis.

angles). Instead, the copper atoms are equivalent in **3**. As in **1**, the four equatorial bonds to the metal atom in **2** and **3** occur in two sets: the copper to hydroxo-bridge oxygen (1.921(4)−1.931(4) Å in **2** and 1.921(3)−1.923(3) Å in **3**) and the copper to bipyrimidyl nitrogen (2.055(5)−2.035(5) Å in **2** and 2.032(4)−

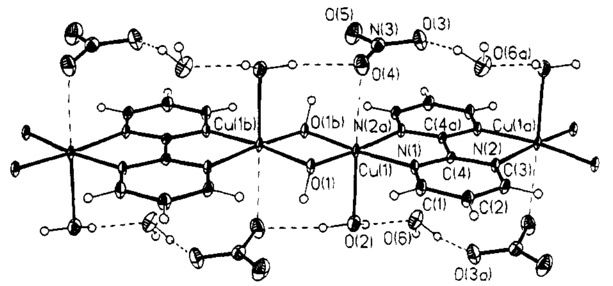

Figure 4. ORTEP view of the alternating chain **4** with the atom-numbering scheme. Thermal ellipsoids are plotted at the 30% probability level.

2.054(4) Å in **3**). The axial Cu−O bonds are significantly larger (2.298(6) and 2.320(7) Å for Cu(1)−O(3) and Cu(2)−O(6) in **2** and 2.326(4) Å for Cu(1)−O(2) in **3**). The largest deviations from the N(1)N(2)O(1)O(2) and N(3)N(4)O(1)O(2) (**2**) and N(1)N(2a)O(1)O(1b) (**3**) equatorial mean planes are 0.076(5), 0.006(5), and 0.023(4) Å, respectively. The copper atoms are displaced from the basal planes by 0.221(1) (Cu(1)) and 0.227(1) Å (Cu(2)) toward the nitrato groups in **2** and by 0.145(1) Å (Cu(1)) toward the coordinated water in **3**. The dihedral angle between the equatorial planes around Cu(1) and Cu(2) in **2** is 6.2(1)°, whereas that referred to Cu(1) and Cu(1a) in **3** is 0°.

Both **2** and **3** grow as linear chains of copper(II) ions, with a regular alternation of bpm and double hydroxo bridges. Two nitrate ligands in *cis* and two water molecules in *trans* arrangement with respect to the (bpm)Cu$(OH)_2$Cu(bpm) mean plane are present in **2** and **3**, respectively. Adjacent pairs of symmetry-equivalent nitrate anions are alternately up and down along the chain in **2**, as shown in Figure 2 (bottom), the nitrate oxygen atoms of one chain pointing toward the copper atoms of the nearest one (Cu(1)···O(4) and Cu(2)···O(8) distances are 2.9 and 3.1 Å, respectively). Two inversion centers, one located at the middle of the C(4)−C(4a) bond and the other halfway between the O(1) and O(1b) distance, impose the up and down arrangement of the adjacent water molecules along the chain in **3**. An extensive network of hydrogen bonds, involving water molecules, hydroxo groups, and nitrate anions (see end of Table 8), links the chains in **3**, as shown in Figure 3 (bottom). In this respect, it deserves to be noted that an oxygen atom (O(3)) of a nitrate anion is linked to three hydrogen atoms (two from water molecules and one from a hydroxo group), conferring a distorted tetrahedral geometry to this oxygen. The presence of two nitrate ligands in a *cis* arrangement in **2** instead of two water molecules in *trans* positions in **3** is related to a larger waving behavior of the chain in **2**.

Compound **4** is very close to **3**, the only difference being the presence of a crystallization water molecule and weakly coordinated nitrate anions. Each copper atom exhibits a distorted 4+1+1 octahedral coordination as in **1**. The equatorial Cu−N(bpm) and Cu−O(hydroxo bridge) bonds average 2.039 and 1.940 Å, respectively (2.016 and 1.944 Å in **1**). The axial Cu(1)−O(2) (2.311(3) Å) and Cu(1)−O(4) (2.721(4) Å) bond distances in **4** are practically identical to the corresponding ones in **1** (2.310(2) and 2.691 (2) Å). The four equatorial atoms are coplanar, with no atom deviating from the least-squares planes by more than 0.005(3) Å. The copper atom is displaced by 0.100(1) Å from this plane toward the O(2) atom of the water molecule. Intra- and interchain hydrogen bonding, involving both coordinated and uncoordinated water molecules and nitrate anions, occurs in **4** (see end of Table 9). The O(4) atom accepts a hydrogen atom from the water molecule linked to the nearby

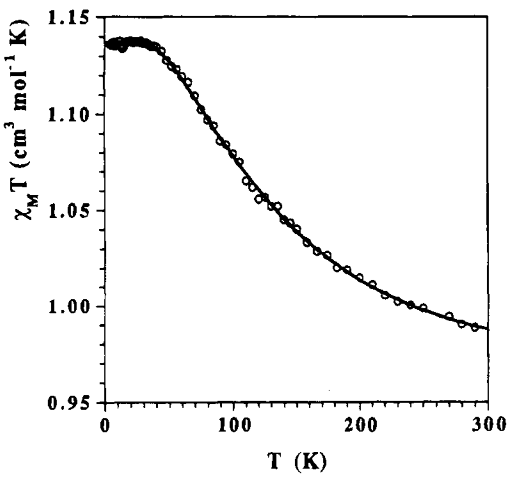

Figure 5. Thermal dependence of $\chi_M T$ for **1**: (O) experimental data; (—) best fitted curve.

copper atom, and the values of the angles around the oxygen suggest that it could also have a distorted tetrahedral geometry.

The bpm bridging ligand, as a whole, is planar in complexes **2**–**4**, and its bond distances and angles are in agreement with those reported in other bpm-bridged copper(II) complexes.[13a,b,24–26] The values of the angle subtended at the copper atom by bpm are 81.8(2) and 81.7(2)° in **2**, 81.4(2)° in **3**, and 81.8(1)° in **4**. The planes of two adjacent bpm ligands form a dihedral angle of 25.6(1)° in **2**, whereas they are parallel in **3** and **4** and separated by 0.269(4) and 0.058(3) Å, respectively.

The metal–metal separations through the double-hydroxo bridge (2.886(1), 2.854(1), and 2.860(1) Å in **2**–**4**, respectively) and the angles at the hydroxo bridge θ (96.2(2) and 96.1(2)° in **2**, 95.9(2)° in **3**, and 95.0(1)° in **4**) are close to those of **1**. The dihedral angle formed by the Cu(1)O(1)O(2) and Cu(2)O(1)O(2) planes in **2** is 167.8(2)°, whereas Cu(1), O(1), O(1b), and Cu(1b) in **3** and **4** lie on a plane. The intrachain metal–metal separations through bpm are 5.471(1) (Cu(1)···Cu(1b)) and 5.474(1) Å (Cu(2)···Cu(2a)) in **2**, 5.461(2) Å (Cu(1)···Cu(1b)) in **3**, and 5.452(2) Å (Cu(1)···Cu(1b)) in **4**. The shortest interchain metal–metal separations are 7.040(1), 6.818(2), and 6.933(2) Å in **2**–**4**, respectively.

Magnetic Properties and EPR Data. The magnetic behavior of compound **1** is shown in Figure 5 in the form of the variation of $\chi_M T$ versus the temperature T, χ_M being the molar magnetic susceptibility for the dinuclear unit. At room temperature $\chi_M T$ is equal to 0.98 cm^3 mol^{-1} K, already higher than what is expected for two uncoupled copper(II) ions. $\chi_M T$ increases smoothly upon cooling and reaches a plateau at 40 K with $\chi_M T$ = 1.14 cm^3 mol^{-1} K, which remains practically constant until 4.2 K. This magnetic behavior corresponds to a triplet ground state with a large energy separation from the excited singlet state. The $\chi_M T$ plateau is obtained in the temperature range when only the ground state is populated. The magnetic susceptibility for this structurally characterized dimer can be expressed as eq 1, where J is the singlet–triplet energy

$$\chi_M = \frac{2N\beta^2 g^2}{kT}[3 + \exp(-J/kT)]^{-1} \qquad (1)$$

gap and N, β, g, and k have their usual meanings. The average value of the g factor for the triplet can be deduced from the value of the plateau ($\chi_M T = 2N\beta^2 g^2/3k$). This gives g = 2.13. The value of J was determined by a least-squares fitting procedure (g was kept constant and equal to 2.13, in the fitting process) looking for the minimum of the factor R defined as $R = \sum[(\chi_M T)^{obsd} - (\chi_M T)^{calcd}]^2/\sum[(\chi_M T)^{obsd}]^2$. Values of 114 cm^{-1} and 4.1×10^{-4} were found for J and R, respectively.

Further evidence for the triplet ground state in **1** is provided by its EPR spectrum. The X-band polycrystalline powder EPR spectra of this compound, up to 12 000 G at 77 K, exhibit five features at 1620, 3150, 6635, 8541, and 10 319 G. The two features at lower field are of low intensity. The spectrum is qualitatively similar to that reported for other ferromagnetically-coupled copper(II) pairs with $D > h\nu$.[9,10i,27–29] The second feature is probably due to a noncoupled copper(II) impurity as suggested by its temperature dependence. When the sample is heated, the absolute intensities of the other four features quickly diminish, supporting the notion of a triplet nature for the ground state. It can be assumed that the peak at lower field corresponds to a component of the $\Delta M_S = \pm 2$ transition (it is the only peak of the lower field region that we have observed in our spectrometer). The presence of the other peaks at high field values is as expected for the case in which the value of the axial zero-field-splitting parameter D is larger than the incident quantum (about 0.3 cm^{-1}). Our attempts to analyze this spectrum in terms of an axial spin Hamiltonian using the equations of Wasserman et al.[30] led to the following values: g_x = 2.05, g_y = 1.98, g_z = 2.10, $|D|$ = 1.38 cm^{-1}, and E = 0.031 cm^{-1}, the peaks at 6635, 8541, and 10 319 G being assigned to H_{x2}, H_{y2}, and H_{z1}, respectively. Although the agreement between observed and calculated [6643 (H_{x2}), 8544 (H_{y2}), and 10 381 G (H_{z1})] fields is very good, the unreasonable value of the g_y component suggests that the **g** and **D** tensors in **1** are probably nonparallel, and consequently, the Wasserman equations cannot be used.

The thermal dependences of χ_M and $\chi_M T$ (χ_M being the magnetic susceptibility per two copper(II) ions) for compounds **2**–**4** are very similar. For the sake of brevity, only the magnetic properties of **4**, χ_M and $\chi_M T$, are shown in Figure 6. At room temperature the value of $\chi_M T$ for **4** is 0.77 cm^3 mol^{-1} K (0.71 and 0.78 cm^3 mol^{-1} K for **2** and **3**, respectively), a value much smaller than that expected for two uncoupled copper(II) ions. This value drops as the temperature decreases and vanishes in the lower temperature region. The susceptibility curves of **2**–**4** exhibit rounded maxima in the temperature range 120–110 K. Magneto–structural data of complex **1** and bpm-bridged copper(II) complexes allow us to foresee alternating antiferromagnetic (through the bpm bridge) and ferromagnetic (through the double-hydroxo bridge) exchange coupling within the chains **2**–**4** as shown in **I**. Consequently, the magnetic data for complexes

$$\begin{array}{ccccccccc} \uparrow & J_{AF} & \downarrow & J_F & \downarrow & J_{AF} & \uparrow & J_F & \uparrow \\ \text{— Cu}_1 & \text{—} & \text{Cu}_2 & \text{—} & \text{Cu}_1 & \text{—} & \text{Cu}_2 & \text{—} & \text{Cu}_1\text{ —} \end{array}$$

I

2–**4** were analyzed with the Hamiltonian $\hat{H} = -J\sum(\hat{S}_{2i}\hat{S}_{2i-1} - \alpha\hat{S}_{2i}\hat{S}_{2i+1})$, where J is the exchange coupling parameter associ-

(24) De Munno, G.; Bruno, G. *Acta Crystallogr., Sect. C* **1984**, *40*, 2030.
(25) Morgan, L. W.; Goodwin, K. V.; Pennington, W. T.; Petersen, J. D. *Inorg. Chem.* **1992**, *31*, 1103.
(26) De Munno, G.; Julve, M.; Verdaguer, M.; Bruno, G. *Inorg. Chem.* **1993**, *32*, 2215.
(27) Jeter, D. V.; Lewis, D. L.; Hempel, J. C.; Hodgson, D. J.; Hatfield, W. E. *Inorg. Chem.* **1972**, *11*, 1958. Barnes, J. A.; Hodgson, D. J.; Hatfield, W. E. *Inorg. Chem.* **1972**, *11*, 144.
(28) Banci, L.; Bencini, A.; Gatteschi, D.; Zanchini, C. *J. Magn. Reson.* **1982**, *48*, 9. Banci, L.; Bencini, A.; Gatteschi, D. *J. Am. Chem. Soc.* **1983**, *105*, 761.
(29) Sikorav, S.; Bkouche-Waksman, I.; Kahn, O. *Inorg. Chem.* **1984**, *23*, 492.
(30) Wasserman, E.; Snyder, L. C.; Yager, W. A. *J. Chem. Phys.* **1964**, *41*, 1763.

Table 10. Selected Magneto–Structural Data for Hydroxo-Bridged Bpm-Containing Copper(II) Complexes[a]

compd	Cu–O, Å	Cu–Cu,[b] Å	Cu–Cu,[c] Å	Cu–O–Cu, deg	OCuO/OCuO, deg	J_F,[d] cm^{-1}	J_{AF},[e] cm^{-1}
1	1.944	2.881		95.7	0.0	+114	
2	1.926	2.886	5.473	96.2	12.2	+105	−140
3	1.922	2.854	5.461	95.9	0.0	+97.5	−135
4	1.940	2.860	5.452	95.0	0.0	+160	−145
5	1.950	2.870		95.0	0.0	+147	

[a] Average bond distances and angles are given for each structure. [b] Metal–metal separation through the double-hydroxo bridge. [c] Metal–metal separation through the bpm bridge. [d] Exchange coupling parameter through the double-hydroxo bridge. [e] Exchange coupling parameter through the bpm bridge.

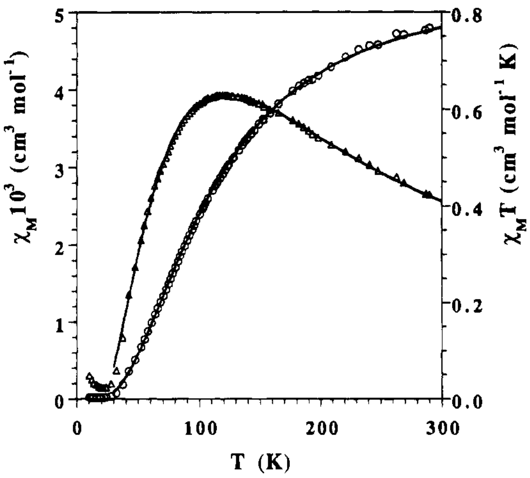

Figure 6. Plot of $\chi_M T$ (○) and χ_M (△) *vs T* for **4**. Solid lines correspond to the best fitted curves.

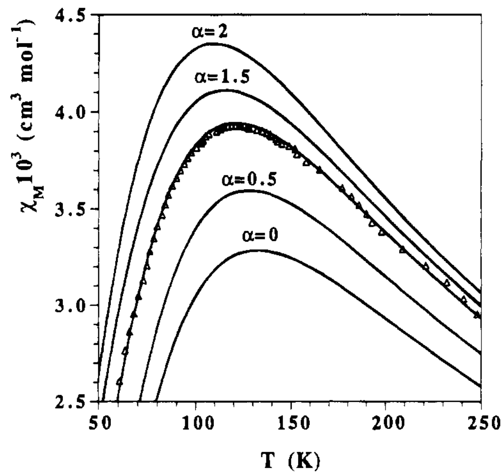

Figure 7. Thermal variation of the susceptibility of **4**: (△) experimental data; (—) theoretical curves (with fixed values of $J_{AF} = -145$ cm^{-1} and $g = 2.13$) obtained for various values of the alternation parameter α.

ated with a particular copper(II) pair and αJ is the exchange constant associated with the adjacent unit (the alternating parameter α being defined as $J_F/|J_{AF}|$). In order to analyze the magnetic data, we used a numerical expression for an alternating ferro- and antiferromagnetic Heisenberg chain derived[31] by Georges et al., which is based on closed spin chains of increasing length (the calculations were limited up to 14-spin rings with S being $^1/_2$). The numerical expression used to fit the experimental data is given in the Appendix. Our data fit this model perfectly (Figure 6). The best-fit parameters J_{AF} and J_F are −140 and 105 cm^{-1} for **2**, −135 and −97.5 cm^{-1} for **3**, and −145 and 160 cm^{-1} for **4** with g values of 2.02 (**2**), 2.11 (**3**), and 2.13 (**4**). The values of R were 3.5×10^{-4}, 3.7×10^{-4}, and 4.0×10^{-5} for **2**–**4**, respectively. The influence of α on the magnetic curve of **4** is illustrated by Figure 7.

Relevant magneto–structural data dealing with complexes **1**–**5** are collected in Table 10. The dinuclear bis(μ-hydroxo) compounds **1** and **5** display a strong intramolecular ferromagnetic coupling, in agreement with Hatfield and Hodgson's correlation[8] between J and the Cu(OH)Cu θ bridging angle. The coupling is ferromagnetic when the θ angle is smaller than 97.5° (95.7 and 95.0° for **1** and **5**, respectively). The fact that the values of the intramolecular copper–copper separation and θ in **5** are smaller than that of **1** accounts for the somewhat larger ferromagnetic coupling found in **5**. This behavior was rationalized by Kahn in terms of accidental orthogonality[32] of the magnetic orbitals ϕ_A and ϕ_B which describe the unpaired electron on each copper(II) ion (ϕ_A and ϕ_B being $d_{x^2-y^2}$ type magnetic orbitals delocalized on the N(1) and N(2) bpm nitrogen and O(1) and O(1a) hydroxo oxygen atoms). The overall overlap integral $S = \langle\phi_A/\phi_B\rangle$ is close to zero around the angle where orthogonality occurs, and the singlet–triplet energy gap, approximated by the expression $J = 2j + 4\beta S$ (j is the bielectronic exchange integral $\langle\phi_A(1)\ \phi_B(2)|e^2/r_{12}|\phi_A(2)\ \phi_B(1)\rangle$), is governed by the positive $2j$ term. This analysis is also pertinent for the μ-hydroxo moiety of the alternating chains **2**–**4**, explaining the ferromagnetic J_F constant. The antiferromagnetic coupling constant J_{AF} arises, as we already demonstrated,[13a,b] from the interaction through the Cu(bpm)Cu fragment thanks to the strong σ in-plane overlap between the $d_{x^2-y^2}$ type magnetic orbitals centered on each copper(II) ion. The values of $-J$ through bpm in **2**–**4** are very similar, as expected from the structural parameters of the Cu(bpm)Cu units.

Concluding Remarks. The present work affords a new strategy to build one-dimensional compounds exhibiting a regular alternation of ferro- and antiferromagnetic couplings, which is based on the use of bis(μ-hydroxo) copper(II) $[(bpm)Cu(OH)_2Cu(bpm)]^{2+}$ dinuclear units as "complex ligands". Taking advantage of the bis-chelating character of bpm, one can obtain ...M(bpm)Cu(OH)$_2$Cu(bpm)M... homo- (present case with M = Cu(II)) and polymetallic (work in progress) chains with an alternating hydroxo–bpm bridging arrangement. Another goal of our studies with the Cu(OH)$_2$Cu framework is the synthesis of alternating chains with $J_F > |J_{AF}|$. In this case, the double-hydroxo-bridged copper(II) unit would behave as a triplet at low temperature and the antiferromagnetic interaction could led to a Haldane gap system[33,34] built from spins $^1/_2$. We are working along these lines in order to explore in more detail this quantum phenomenon.

Acknowledgment. This work was finantially supported by the Dirección General de Investigación Científica y Técnica

(31) (a) Borrás-Almenar, J. J.; Coronado, E.; Curely, J.; Georges, R.; Gianduzzo, J. J. *Inorg. Chem.* **1994**, *33*, 5171. (b) Borrás-Almenar, J. J. Ph.D. Thesis, University of València, 1992.
(32) Kahn, O.; Charlot, M. F. *Nouv. J. Chim.* **1980**, *4*, 567.
(33) Haldane, F. D. M. *Phys. Lett.* **1983**, *A93*, 464; *Phys. Rev. Lett.* **1983**, *50*, 1153.
(34) Gadet, V.; Verdaguer, M.; Briois, V.; Gleizes, A. *Phys. Rev.* **1991**, *B44*, 705. Takeuchi, K.; Hori, H.; Date, M.; Yosida, T.; Katsumata, K.; Renard, J. P.; Gadet, V.; Verdaguer, M. *J. Magn. Magn. Mater.* **1992**, *104–107*, 813.

(DGICYT) (Spain) through Project PB91-087-C02-01, the Italian Ministero dell'Università e della Ricerca Scientifica e Tecnologica, the Spanish-French Integrated Actions, and the Human Capital and Mobility Program (Network on Magnetic Molecular Materials from EEC) through Grant ERBCHRX-CT920080.

Appendix

The value of χ_M (magnetic susceptibility per two copper(II) ions) is calculated through the equations

$$\chi_M = \frac{N\beta^2 g^2}{2kT} F(\alpha,x) \tag{A1}$$

$$F(\alpha,x) = \frac{A_1x^4 + A_2x^3 + A_3x^4 + A_4x}{x^4 + A_5x^3 + A_6x^2 + A_7x + A_8} \tag{A2}$$

$$\alpha = \frac{J_F}{|J_{AF}|} \tag{A3}$$

$$x = \frac{kT}{|J_{AF}|} \tag{A4}$$

The values of the coefficients A_n in eq A2 are calculated through the equation

$$A_n = \sum_{i=0}^{i=3} a_{ni}\alpha^i \tag{A5}$$

and the corresponding a_{ni} values, valid in the range $0 \le \alpha \le 5$, are as follows:

	$i = 0$	$i = 1$	$i = 2$	$i = 3$
$n = 1$	1	0	0	0
$n = 2$	5	0	0	0
$n = 3$	−1	0	0	0
$n = 4$	0.5	0	0	0
$n = 5$	5.32559	−1.15923	0.34561	−0.03731
$n = 6$	0.49591	−0.01920	−0.01617	−0.00795
$n = 7$	0.03123	0.48241	−0.16542	0.01445
$n = 8$	0.33563	−0.34155	0.09592	−0.00846

Supplementary Material Available: Tables of data collection information, anisotropic temperature factors, hydrogen atom coordinates, bond lengths and angles, and least-squares planes and figures showing the arrangement of chains in **3** along the *b* axis and plots of $\chi_M T$ and χ_M vs T for **2** and **3** (23 pages). Ordering information is given on any current masthead page.

IC941022N